

From multivariate time series to multiplex visibility graphs

Vincenzo Nicosia, Lucas Lacasa, and Vito Latora

School of Mathematical Sciences, Queen Mary University of London, Mile End Road, E14NS London, UK

We introduce a method to transform multivariate time series into multiplex networks, and we illustrate how to extract important information on high dimensional dynamical systems from the topological analysis of the derived networks. In particular, we focus on both diffusively and globally coupled chaotic maps, showing that multiplex measures such as the interlayer mutual information accurately describe and quantify: (i) the information flow among degrees of freedom, (ii) the transition between different dynamical phases, and (iii) the onset of various types of synchronization. The method is general and scalable, and can be efficiently used for the analysis of multivariate time series deriving from physical, biological or socio-economic systems.

PACS numbers: 89.75.Hc, 05.45.Tp, 89.75.Fb, 05.45.Ra

Time series analysis is a central topic in physics, as well as a general and powerful method to characterize data in biology, medicine and economics, and to understand their underlying dynamical origin. In the last decades, the topic has received input from different disciplines such as nonlinear dynamics, statistical physics, computer science or Bayesian statistics and, as a result, new approaches like nonlinear time series analysis [1] or data mining [2] have emerged. More recently, the science of complex networks [3–5] has fostered the growth of a novel approach to time series analysis based on the transformation of a time series into a network according to some specified mapping algorithm, and on the subsequent extraction of information on the time series through the analysis of the derived network [6–11].

Among others approaches, the so called visibility algorithms [10, 11] have been shown to be simple, computationally efficient and analytically tractable methods to transform univariate time series into graphs [12, 13], able to extract nontrivial information about the original signal [14], classify different dynamical origins [15] and provide a clean description of low dimensional dynamics [16–18]. As a consequence, these methods have been used in different domains including earth and planetary sciences [19–21], finance [22] or biomedical fields [23] (see [24] for a complete review). Despite their success, the range of applicability of these methods is only limited to univariate time series, whereas the most challenging problems in several areas of physics and nonlinear science concern systems governed by a large number of degrees of freedom, whose evolution is indeed described by multivariate time series.

For this reason, in this Article we introduce a visibility approach to analyze multivariate time series based on the mapping of a multidimensional signal into an appropriately defined multi-layer network [25–30], which we call *multiplex visibility graph*. We validate our method by addressing concrete problems in nonlinear dynamics, showing that the multiplex visibility graph is indeed a natural and well-defined setting for representing and retrieving information from high dimension dynamical systems in a

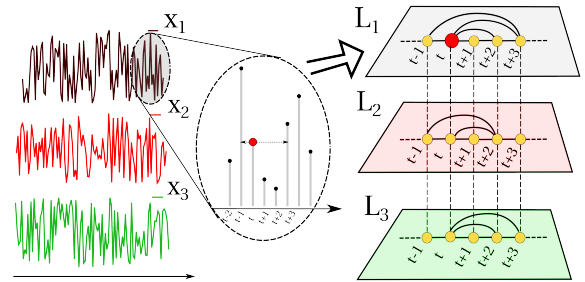


FIG. 1. (color online) We use the Horizontal Visibility Graph (HVG) algorithm to map a M -dimensional time series into the *multiplex visibility graph* \mathcal{M} , a multi-layer network where each layer α is the HVG of the time series $\{x^{[\alpha]}(t)\}_{t=1}^N$.

simple, accurate and computationally efficient way.

We start by recalling that visibility algorithms are a family of geometric criteria which define different ways of mapping an ordered series, for instance a temporal series of N real-valued data $\{x(t)\}_{t=1}^N$, into a graph of N nodes. For instance, in the horizontal version of the algorithm, the so-called Horizontal Visibility Graph (HVG), two nodes i and j are linked by an undirected edge if the associated data $x(i)$ and $x(j)$ have horizontal visibility, i.e. if every intermediate datum $x(k)$ satisfies the relation [11]:

$$x(k) < \inf\{x(i), x(j)\}, \quad \forall k : i < k < j. \quad (1)$$

This algorithm has been extended in various ways, by relaxing the visibility criterion [10], and has also been employed to construct directed visibility graphs –by distinguishing ingoing from outgoing links with respect to the arrow of time– which have proven useful to assess time asymmetries and to quantify time series irreversibility [31, 32]. Here, we propose the following method to construct visibility graphs able to deal with multivariate series. Without any loss of generality, let us consider a M -dimensional real valued time series $\{\mathbf{x}(t)\}_{t=1}^N$, with $\mathbf{x}(t) = (x^{[1]}(t), x^{[2]}(t), \dots, x^{[M]}(t)) \in \mathbb{R}^M$ for any value of t , extracted from a M -dimensional, either deterministic

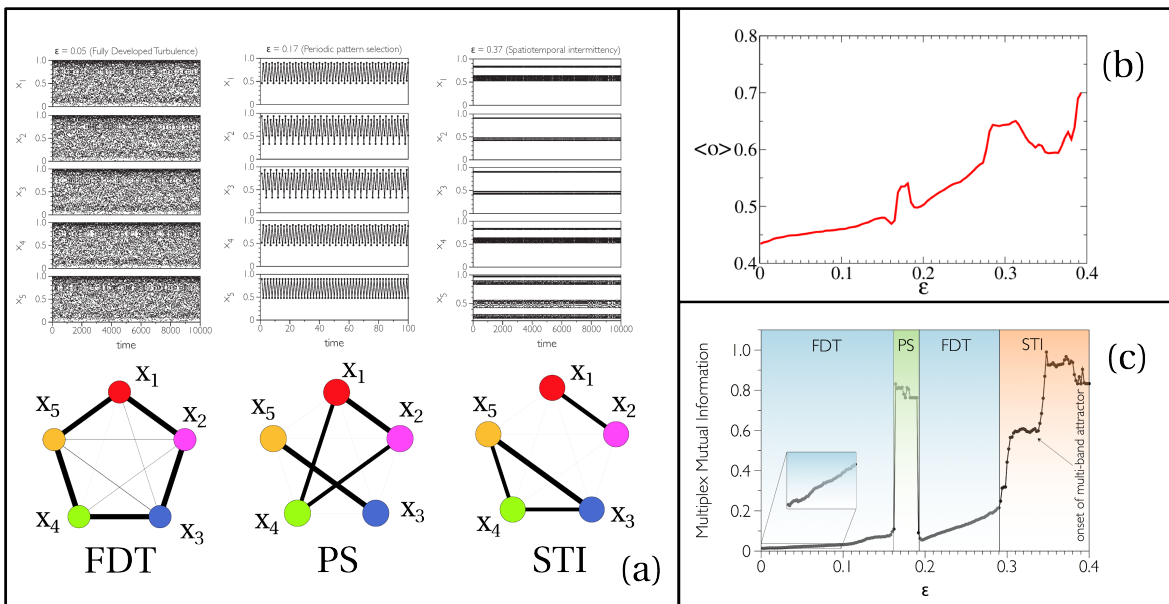


FIG. 2. (color online) (a) Sample time series generated by five diffusively coupled fully chaotic logistic maps at different values of the coupling strength ϵ , showing Fully Developed Turbulence (FDT) at $\epsilon \simeq 0.05$, Pattern Selection (PS) at $\epsilon \simeq 0.17$, and Spatio-temporal Intermittency (STI) at $\epsilon \simeq 0.37$. Information flow among units is well captured by projecting the multiplex visibility graph \mathcal{M} into a graph of layers \mathcal{G} (bottom of the panel), where each node represents a layer and the weight of an edge is given by the mutual information among the two layers. (b) The average edge overlap $\langle o \rangle$ and (c) the pairwise averaged mutual information I of the associated multiplex visibility graph can be used as order parameters to distinguish different dynamical phases.

or stochastic, dynamical system $\mathbf{x}(t+1) = \mathbf{F}(\mathbf{x}(t))$. We can construct the HVG associated to the time series of each state variable $\{x_i^{[\alpha]}(t)\}_{i=1}^N$, and we can consider a M -layer multiplex network, where each of the layers corresponds to one of the M HVGs. As an example, the procedure to map a 3-dimensional time series into a 3-layer multiplex visibility graph is illustrated in Fig. 1. Clearly, the multiplex version of different types of visibility graphs, other than the HVG, can be constructed by using analogous procedures, and in every case the time complexity is linear in the number of layers, yielding an efficient and scalable class of algorithms. The structure of the *multiplex visibility graph* \mathcal{M} derived in this way is described by the vector of adjacency matrices of its layers $\mathcal{A} = \{A^{[1]}, A^{[2]}, \dots, A^{[M]}\}$, where $A^{[\alpha]} = \{a_{ij}^{[\alpha]}\}$ and $a_{ij}^{[\alpha]} = 1$ if and only if node i and node j are connected by a link at layer α [26, 30]. Then, a variety of structural indicators, recently introduced in the literature to characterize the structure of multiplex networks [25, 27–30, 33, 34], can be used to extract useful information on the original multivariate time series. In particular, in this work we focus on a couple of multiplex measures which allow to quantify the information flow across degrees of freedom of the underlying high dimensional system. The first of this quantities is the so called *average edge overlap*

$\langle o \rangle$ defined as:

$$\langle o \rangle = \frac{1}{\mathcal{K}} \sum_{i,j} o_{ij}, \quad o_{ij} = \frac{1}{M} \sum_{\alpha} a_{ij}^{[\alpha]} \quad (2)$$

where o_{ij} is the overlap of the edges between node i and node j at the different layers, and \mathcal{K} is the total number of pairs of nodes connected on at least one of the M layers [30]. Notice that $o_{ij} = 0$ if $a_{ij}^{[\alpha]} = 0 \forall \alpha$, while it takes its maximum $o_{ij} = 1$ when nodes i and j are connected at each of the M layers. Consequently, the more similar are the connection patterns of the layers of \mathcal{M} and, in turn, the structure of the corresponding time series, the higher $\langle o \rangle$, with $\langle o \rangle = 1$ if and only if all the layers are identical, i.e. if the original M -dimensional time series can be effectively reduced to a 1-dimensional one.

The second measure we make use of aims at quantifying the presence of inter-layer degree correlations [34]. Given a pair of layers α and β of \mathcal{M} , respectively characterized by the degree distributions $P(k^{[\alpha]})$ and $P(k^{[\beta]})$, we define the *interlayer mutual information* $I_{\alpha,\beta}$:

$$I_{\alpha,\beta} = \sum_{k^{[\alpha]}} \sum_{k^{[\beta]}} P(k^{[\alpha]}, k^{[\beta]}) \log \frac{P(k^{[\alpha]}, k^{[\beta]})}{P(k^{[\alpha]})P(k^{[\beta]})} \quad (3)$$

where $P(k^{[\alpha]}, k^{[\beta]})$ is the joint probability to find a node having degree $k^{[\alpha]}$ on layer α and degree $k^{[\beta]}$ on layer

β . In general, the higher $I_{\alpha,\beta}$ the more correlated the degree distributions of the two layers and, therefore, the structure of the associated time series. If we average the quantity $I_{\alpha,\beta}$ over every possible pair of layers of \mathcal{M} , we obtain a scalar variable $I = \langle I_{\alpha,\beta} \rangle_{\alpha,\beta}$ which coarse-grains the amount of information flow in the system. Note also that the values $\{I_{\alpha,\beta}\}$ can be considered as the weights of the edges of the *graph of layers* \mathcal{G} , this being a projection of the original multiplex visibility graph \mathcal{M} into a (monoplex) weighted graph with M nodes, where each node represents one layer, and the edges represent correlations between layers.

Information flow and phase diagram in CMLs. — As a first case study we consider diffusively coupled map lattices (CMLs), M -dimensional dynamical systems with discrete time, discrete space, and continuous state variables, widely used to model complex spatio-temporal dynamics [35]. We focus here on a ring of M sites, and we assume that the dynamical evolution of state $x^{[\alpha]}$ of site α is determined by:

$$x^{[\alpha]}(t+1) = (1-\epsilon)f[x^{[\alpha]}(t)] + \frac{\epsilon}{2} \left(f[x^{[\alpha-1]}(t)] + f[x^{[\alpha+1]}(t)] \right), \quad (4)$$

$\forall \alpha = 1, \dots, M$, where $\epsilon \in [0, 1]$ is the coupling strength, and $f(x)$ is typically a chaotic map [36]. For different values of ϵ and M CMLs display a very rich phase diagram, which includes different degrees of coherence and dynamical phases such as Fully Developed Turbulence (FDT, a phase with incoherent spatiotemporal chaos), Pattern Selection (PS, a sharp suppression of chaos in favor of a randomly selected periodic attractor), or different forms of spatio-temporal intermittency (STI, see Ref. [35] for a comprehensive review). The origin of such a rich structure comes from the interplay between the local tendency towards inhomogeneity, induced by the chaotic dynamics, and the global tendency towards homogeneity in space, induced by the diffusive coupling. In Fig. 2 we consider a simple example of a CML consisting of $M = 5$ diffusively coupled, fully chaotic logistic maps $f(x) = 4x(1-x)$, which exhibits several transitions from incoherent chaos, to pattern selection, to several forms of synchronized chaos when ϵ is increased. In particular, the spatio-temporal coherence of the system is an increasing function of the coupling in the FDT regime and reaches larger values for partially or fully synchronized states. The characterization of the different phases is usually performed through a set of numerical methods [35], some of which deal with patterns formed by an arbitrary number of symbols, where each symbol is produced by partitioning the phase space into an arbitrary number of cells (usually two) and coarse-graining the trajectories accordingly. In Fig. 2(b) and 2(c) we show that, both the average edge

overlap $\langle o \rangle$ and the average mutual information I of the multiplex visibility graph associated to the system, are able to distinguish between the different phases [37]. In particular, I is a monotonically increasing function of ϵ in the FDT phases, and therefore quantifies the amount of information flow among units. Notably, it also detects qualitative changes in the underlying dynamics (such as the chaos suppression in favor of a randomly selected periodic pattern, or the onset of a multi-band chaotic attractor during intermittency) and therefore can be used as a scalar order parameter of the system. In the panel (a) of the same figure we have also represented the projection of the multiplex \mathcal{M} into the graph of layers \mathcal{G} of the system, where the width of each edge is proportional to the value of mutual information between the corresponding layers. A simple visual inspection allows to identify the different kinds of information flow among units in the different dynamical phases.

Scaling up the system. — The previous study suggests that the quantities $\{I_{\alpha,\beta}\}$ (see Fig. 2(a)) accurately capture relevant information of the underlying dynamics. To further explore this aspect and to assess scalability, we considered a ring of $M = 200$ diffusively coupled logistic maps, each governed by Eq. (4). New dynamical phases, such as the so called Brownian motion of Defects (BD) —a transient phase between FDT and PS—, emerge when the dimension of the system is increased, and as the description gets more cumbersome, projections and coarse-grained variables are needed [35]. Since the graph of layers \mathcal{G} is by construction a complete graph, in Fig. 3 we report the structural properties of \mathcal{G}' , the backbone of \mathcal{G} obtained starting from an empty graph of M nodes and adding edges sequentially in decreasing order of $I_{\alpha,\beta}$, until the resulting graph consists of a single connected component [38]. The structure of \mathcal{G}' varies across different dynamical phases, thus providing a simple qualitative way to portrait different dynamics in high-dimensional systems.

Onset of full coherence in GCMs. — Finally, we consider a system of Globally Coupled Maps (GCMs) [39]:

$$x^{[\alpha]}(t+1) = (1-\epsilon)f[x^{[\alpha]}(t)] + \frac{\epsilon}{M} \sum_{\beta \neq \alpha} f[x^{[\beta]}(t)] \quad (5)$$

$\forall \alpha = 1, \dots, M$, where the dynamics of each unit is governed by the logistic map $f(x) = \mu x(1-x)$, $\mu \in [0, 4]$. This system can be indeed considered as a mean-field version of CMLs. In particular we consider values of μ for which each map is chaotic, i.e. $\mu > \mu_\infty = 3.56995\dots$, excluding periodic windows. In those cases, full coherence of the GCM is only reached when the system is in the simplest chaotic attractor, where $x^{[\alpha]} = x^{[\beta]} \forall \alpha, \beta$, and the dynamics effectively reduces to that of a single logistic map. It can be proved that this is indeed the

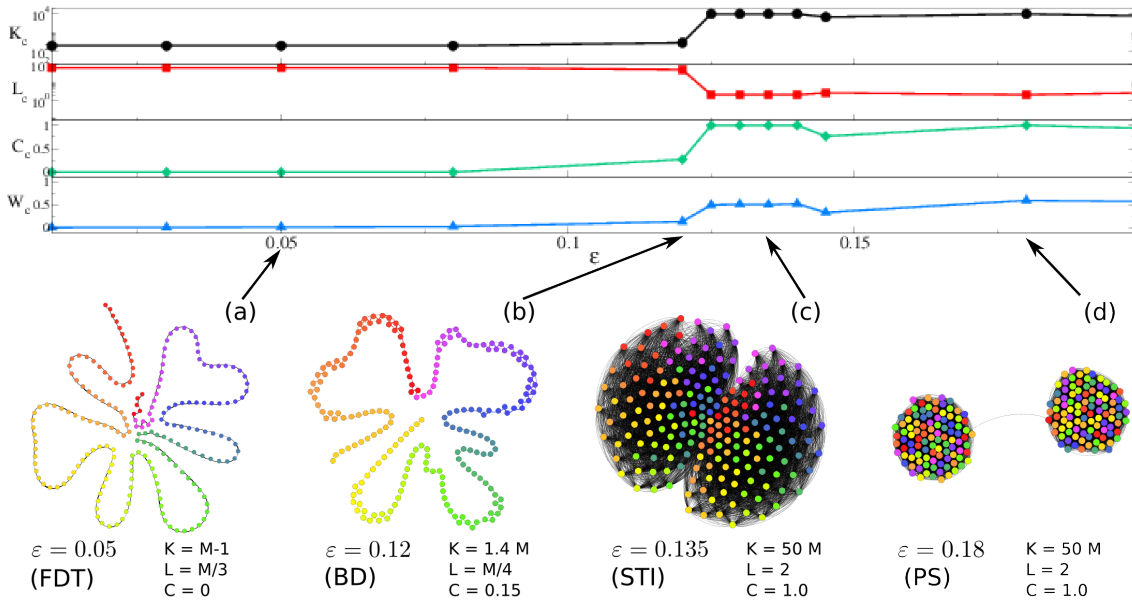


FIG. 3. (color online) The backbone \mathcal{G}' of the graph of layers \mathcal{G} obtained from the multiplex visibility graph of $M = 200$ diffusively coupled chaotic maps for different values of ϵ . Each dynamical phase corresponds to a backbone graph with different structure. We also report several topological properties of \mathcal{G}' (number of edges K , average shortest path length L , clustering coefficient C , and total weight of the edges).

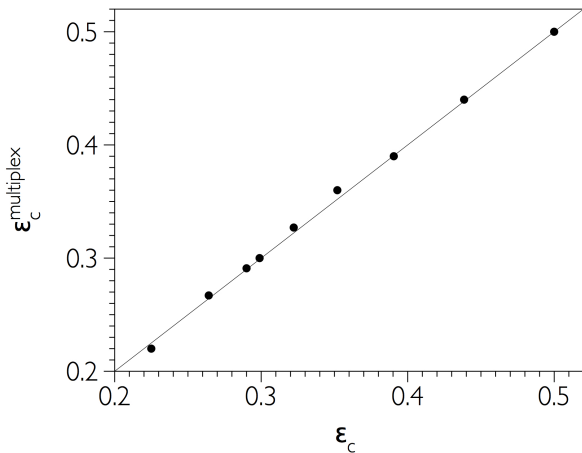


FIG. 4. Scatter plot of the critical value of the coupling strength for the onset of full chaotic coherence, as predicted by the multiplex visibility graph $\epsilon_c^{\text{multiplex}}$, versus the theoretical value ϵ_c .

stable regime for those values of ϵ for which the Lyapunov exponent λ_0 of one isolated logistic map satisfies the inequality $\lambda_0 + \log(1 - \epsilon) < 0$ [39]. The onset of full coherence is therefore reached at a critical value of the coupling strength $\epsilon_c = 1 - \exp(\lambda_0)^{-1}$. For example at $\mu = 4$, by making use of the analytic expression $\lambda_0 = \log 2$, we get that the onset of coherence occurs at $\epsilon_c = 1/2$, whereas for other values of μ the value of

ϵ_c can be derived from the numerical evaluation of the Lyapunov exponent λ_0 . We now show that the multiplex visibility graph approach is able to predict the position of the onset of full coherence. We conjecture that the average mutual information I attains its maximum at the onset of full coherence, and accordingly we propose the quantity $\epsilon_c^{\text{multiplex}} \equiv \min_{\epsilon}(\text{argmax}(I(\epsilon)))$ as a measure of ϵ_c . In Fig. 4 we plot $\epsilon_c^{\text{multiplex}}$ versus ϵ_c for a system of 5 globally coupled chaotic maps and for different values of $\mu \in [\mu_{\infty}, 4]$, finding a remarkable agreement in every case.

Summing up, multiplex visibility graphs provide a novel, accurate and easily scalable approach for multivariate time series analysis. In this work we have focused on signals whose underlying dynamical system is known, showing that dynamical aspects such as information flow, synchronization, and transitions between different dynamical regimes are captured by the computation of some basic multiplex measures. The same approach can be used to study multivariate time series whose precise underlying dynamics is poorly understood or unknown, giving the method a much broader scope and a wider potential applicability.

V.N. and V.L. acknowledge support from the Project LASAGNE, Contract No.318132 (STREP), funded by the European Commission.

-
- [1] H. Kantz and T. Schreiber, *Nonlinear Time Series Analysis* (Cambridge University Press 2006).
- [2] T. Hastie, R. Tibshirani and J. Friedman, *Elements of Statistical Learning* (Springer-Verlag 2009).
- [3] R. Albert and A.-L. Barabasi, *Rev. Mod. Phys.* **74**, 47 (2002).
- [4] S. Boccaletti, V. Latora, Y. Moreno, M. Chavez, D.U. Hwang, *Phys. Rep.* **424**, 175 (2006).
- [5] M.E.J. Newman, *Networks: An Introduction*, Oxford University Press 2010.
- [6] J. Zhang and M. Small, *Phys. Rev. Lett.* **96**, 238701 (2006).
- [7] X. Xu, J. Zhang, and M. Small, *Proc. Natl. Acad. Sci. USA* **105**, 19601 (2008).
- [8] R. V. Donner, Y. Zou, J. F. Donges, N. Marwan, and J. Kurths, *New J. Phys.* **12**, 033025 (2010).
- [9] R. V. Donner et al., *Eur. Phys. J. B* **84**, 653 (2011).
- [10] L. Lacasa, B. Luque, F. Ballesteros, J. Luque, J.C. Nuno, *Proc. Natl. Acad. Sci. USA* **105**, 13 (2008).
- [11] B. Luque, L. Lacasa, J. Luque, F.J. Ballesteros, *Phys. Rev. E* **80**, 046103 (2009).
- [12] L. Lacasa, *Nonlinearity* **27**, 2063-2093 (2014).
- [13] G. Gutin, M. Mansour, S. Severini, *Physica A* **390**, 12 (2011).
- [14] L. Lacasa, B. Luque, J. Luque and J.C. Nuño, *Europhys. Lett.* **86**, 30001 (2009).
- [15] L. Lacasa, R. Toral, *Phys. Rev. E* **82**, 036120 (2010).
- [16] B. Luque, L. Lacasa, F.J. Ballesteros, A. Robledo, *Chaos* **22**, 013109 (2012).
- [17] B. Luque, F. J. Ballesteros, A. M. Nunez and A. Robledo, *J. Nonlin. Sci.* **23** (2013).
- [18] A. Nunez, B. Luque, L. Lacasa, J. P. Gomez, A. Robledo *Phys. Rev. E* **87**, 052801 (2013).
- [19] B. Aguilar-San Juan, L. Guzman-Vargas, *Eur. Phys. J. B* **86**, 454 (2013).
- [20] R.V. Donner and J.F. Donges, *Acta Geophysica* **60**, 589-623 (2012),
- [21] Y. Zou, M. Small, Z. Liu, and J. Kurths, *New J. Phys.* **16** (2014).
- [22] M-C Qian, Z-Q Jiang, and W-X Zhou, *J. Phys. A* **43** 335002 (2010).
- [23] M. Ahmadi, K. Ahmadi, M. Rezazade, E. Azad-Marzabadi, *Clinical Neurophysiology* **124**, 6 (2013).
- [24] A. Nuñez, L. Lacasa, B. Luque, Visibility algorithms: a short review in *Graph Theory* (Intech, 2012).
- [25] G. Bianconi, *Phys. Rev. E* **87**, 062806 (2013)
- [26] V. Nicosia, G. Bianconi, V. Latora, M. Barthelemy, *Phys. Rev. Lett.* **111**, 058701 (2013).
- [27] M. De Domenico et al. *Phys. Rev. X* **3**, 041022 (2013).
- [28] M. Kivelä et al. *J. Complex Networks*, doi: 10.1093/comnet/cnu016, *in press* (2014).
- [29] S. Boccaletti, et al. *Phys. Rep.* doi: 10.1016/j.physrep.2014.07.001, *in press* (2014).
- [30] F. Battiston, V. Nicosia, V. Latora, *Phys. Rev. E* **89**, 032804 (2014).
- [31] L. Lacasa, A. Nuñez, E. Roldan, J.M.R. Parrondo, B. Luque, *Eur. Phys. J. B* **85**, 217 (2012).
- [32] J.F. Donges, R.V. Donner and J. Kurths, *Europhys. Lett.* **102**, 10004 (2013).
- [33] V. Nicosia, G. Bianconi, V. Latora, M. Barthelemy, Non-linear growth and condensation in multiplex networks, arXiv:1312.3683 (2013).
- [34] V. Nicosia, V. Latora, Measuring and modelling correlations in multiplex networks, arXiv:1403.1546 (2014).
- [35] K. Kaneko, *Physica D* **34**, 1-41 (1989).
- [36] The notation of Eq. 4 is based on the assumption that sums and differences are performed modulo M , so that $\alpha - 1 = M$ when $\alpha = 1$ and $\alpha + 1 = 1$ when $\alpha = M$
- [37] The plots of Fig. 2 are obtained by averaging over 100 realisations of the CML dynamics. For each realisation, we constructed a multivariate time series $\{\mathbf{x}_1, \mathbf{x}_2, \dots, \mathbf{x}_N\}$ of $N = 2^{14}$ data points (discarding the transient) and we generated the corresponding multiplex visibility graph.
- [38] The graph obtained by using this procedure coincides with \mathcal{G} at the bond percolation threshold, when edge selection is made in decreasing order of weight. Note that other pruning algorithms would yield different topologies for \mathcal{G}' , and that the optimal one might depend on the specific property under study.
- [39] K. Kaneko, *Physica D* **41**, 137-172 (1990).